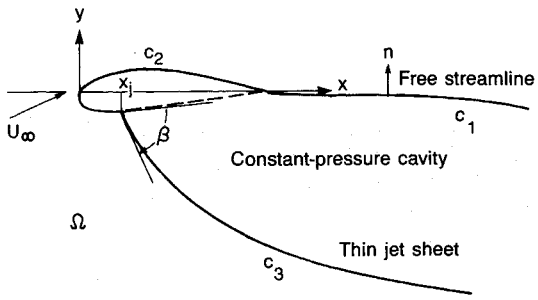

Fig. 1 Inviscid mathematical model.

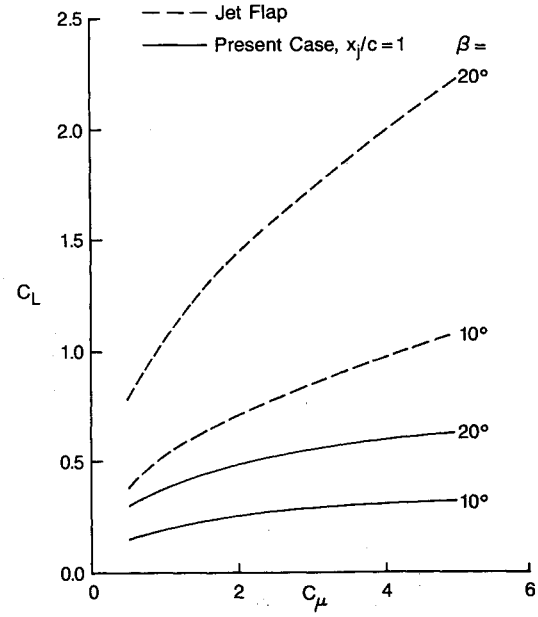

Fig. 2 Comparison with jet flap.

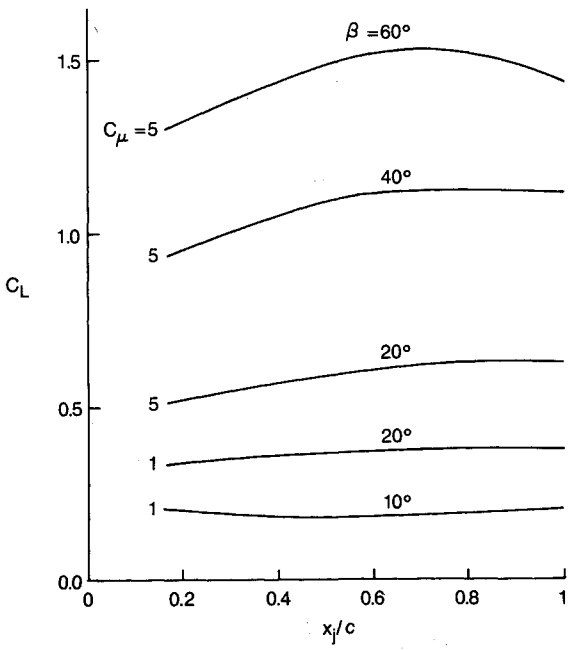

Fig. 3 Effect of jet location on induced lift.

defined as follows:

$$F(q) = |\text{abs}(\nabla\Phi + U_\infty) - \text{abs}(U_\infty)| + \left| \frac{(\nabla\Phi + U_\infty)^2}{U_\infty^2 + \kappa C_\mu - 1} \right| \tag{5}$$

where $| \; |$ denotes the square norm integrated along c_1 and c_2. The function $F(q)$ is minimized through a nonlinear unconstrained optimization algorithm. The results that follow are for a symmetrical, 10% thick airfoil having an elliptical nose over 25% of the chord, and two parallel sides otherwise. Such an airfoil has a blunt trailing edge immersed in the deadwater domain. Figure 2 shows the lift produced by the present concept with the jet located at the trailing edge, as well as the lift produced by the classical trailing edge jet flap. β is the jet ejection angle, as shown in Fig. 1. The lift shown here is that induced by the aerodynamic forces alone and does not include the vertical component of the jet momentum flux. In this configuration, the present concept retains a semi-infinite wake starting at the trailing edge. Clearly, the jet flap is more efficient as a lift augmenting device. Figure 3 describes the evolution of lift for different jet locations along the lower surface, with location parameters defined in Fig. 1. For moderate jet deflection angles, the aerodynamic lift is almost independent of the jet location.

References

[1]Woods, L.C., *The Theory of Subsonic Plane Flow,* Cambridge University Press, Cambridge, England, 1961, pp. 430–431.

[2]Agarwal, R.K. and Deese, J.E., "Euler Solutions for Airfoil/Jet/Ground-Interaction Flowfields," *Journal of Aircraft,* Vol. 23, May 1986, pp. 376–381.

[3]Krothapali, A., Leopold, D., and Koenig, D., "An Experimental Investigation of Flow Surrounding an Airfoil with a Jet Exhausting from Lower Surface," NASA CR-166131, 1981.

[4]Tavella, D.A., Lee, C.S., Wood, N.J., and Roberts, L., "The Jet Spoiler as a Yaw Control Device," AIAA Paper 86-1806, June 1986.

Hypervelocity Gliding Maneuvers

Michael E. Tauber*
NASA Ames Research Center
Moffett Field, California

Nomenclature

A	= reference area of entry vehicle
C_D	= drag coefficient
C_L	= lift coefficient
D	= drag
g	= acceleration of gravity
L	= lift
ℓ	= lateral distance traversed during turn
m	= vehicle mass
R_0	= planetary radius (6367 km for Earth)
s	= longitudinal distance traversed following maneuver
t	= time

Received March 9, 1987.

*Research Scientist. Associate Fellow AIAA.

V = flight velocity
V_f = velocity at end of turn
V_i = velocity at beginning of turn
V_s = circular satellite speed (7.9 km/s)
Y = side force
γ = flight path angle
ρ = freestream density
ϕ = bank or roll angle
ψ = turn angle

Introduction

THE ability to maneuver within the atmosphere during orbital return is a major advantage of high-lift vehicles. For example, a maximum lift/drag ratio of nearly 2 affords the Space Shuttle orbiter a choice of several landing sites. In addition, the Shuttle can be rolled during entry while still maintaining a shallow glide trajectory. This roll maneuver during entry reduces the descent time and, therefore, the total heat input, although the heating rate is increased.[1] One typical measure of maneuvering capability is the maximum lateral range that a vehicle can achieve; the solution to this problem was originally given in Refs. 1 and 2 and refined in Ref. 3. Another important maneuver consists of performing turns that change the vehicle's heading. This Note contains a brief analysis of turning maneuvers during gliding flight, including lateral distances traversed, at velocities up to circular satellite speed.

Analysis

A vehicle maneuvers by rotating the lift vector, thus generating a side force Y. The expression for the side force is

$$Y = L\sin\phi = mV\frac{d\psi}{dt} \tag{1}$$

where ϕ is the roll, or bank, angle and ψ the heading angle. Resolving forces tangential to the flight path gives

$$D - mg\sin\gamma = -m\frac{dV}{dt} \tag{2a}$$

which, for shallow gliding flight, reduces to

$$D = -m\frac{dV}{dt} \tag{2b}$$

Combining Eqs. (1) and (2b) yields

$$d\psi = -\frac{L}{D}\sin\phi\frac{dV}{V} \tag{3a}$$

which, for constant $(L/D)\sin\phi$, integrates to

$$V = V_i - \exp\left\{\frac{2\psi}{[(L/D)\sin\phi]}\right\} - 1\Bigg] \tag{3b}$$

where V_i is the velocity at which the maneuver begins. Vehicles with adequate lift at high speeds typically follow an equilibrium glide trajectory.[4] A spherical, nonrotating planet is assumed and the flight altitude is much less than the planetary radius. In that case, summing the vertical forces in banked flight gives

$$L\cos\phi = mg - \frac{mV^2}{R_0} \tag{4a}$$

The atmospheric density at the flight altitude comes directly from Eq. (4a) and is

$$\rho = \frac{2}{R_0}\frac{m}{C_DA}\frac{1}{L/D\cos\phi}\left(\frac{V_s^2}{V^2} - 1\right) \tag{4b}$$

where V_s is the circular satellite speed $(V_s = gR_0)^{1/2}$. Combining Eqs. (3b) and (4b) yields

$$\rho = \frac{2}{R_0}\frac{m}{C_DA}\frac{1}{L/D\cos\phi}\left[\left(\frac{V_s}{V_i}\right)^2\exp\left\{\frac{2\psi}{[(L/D)\sin\phi]}\right\} - 1\right] \tag{5}$$

The bank angle depends on the criterion that is stipulated for the maneuver; for example, determination of a constant value of the bank angle that maximizes the lateral range.[3] Assume here that the altitude at the conclusion of the turn is to be maximized. In that case, Eq. (5) is differentiated with respect to the bank angle and the result is equated to zero, giving

$$\left[1 - \frac{2\psi}{(L/D)\tan^2\phi\sin\phi}\right]\left(\frac{V_s}{V_i}\right)^2 \times \exp\left\{\frac{2\psi}{[(L/D)\sin\phi]}\right\} - 1 = 0 \tag{6}$$

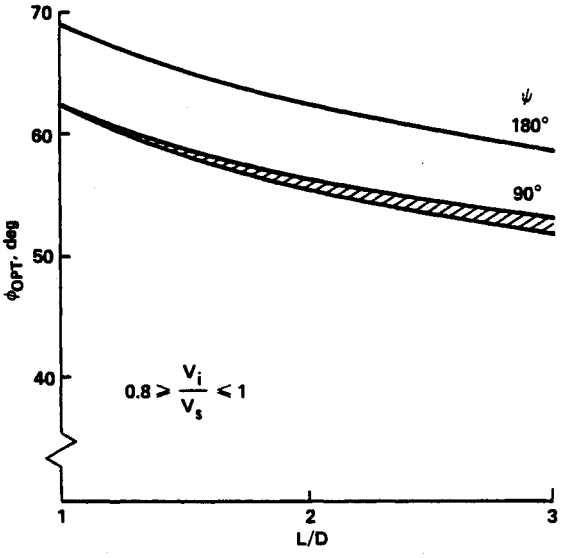

Fig. 1 Variation of optimum bank angle with lift/drag ratio.

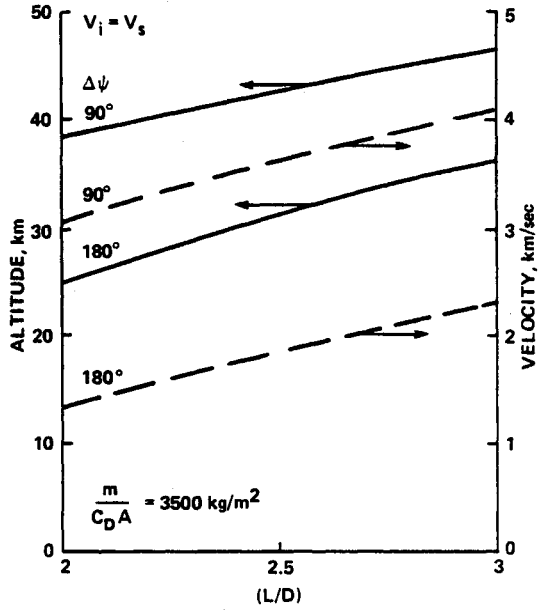

Fig. 2 Flight conditions at end of 90 and 180 deg turns.

Table 1 Distances traversed during and after 90 and 180 deg turns as function of L/D

	Lateral range during turn, km		Residual range after turn, km	
L/D $\Delta\psi=$	90 deg	180 deg	90 deg	180 deg
2.0	3140	3050	1040	186
2.5	4210	4510	1920	454
3.0	5800	6090	3020	860

The optimum bank angle is found for turns of 90 and 180 deg by solving Eq. (6) for a range of lift/drag ratios. The resulting angles are shown in Fig. 1. For initial turning velocities ranging from 0.8 V_s to V_s, the optimum bank angle is insensitive to V_i.

The optimum bank angles are now used to calculate the altitudes and velocities at the conclusion of 90 and 180 deg turns. The turns are initiated upon entry at circular satellite speed ($V_i = V_s$) and are made at constant lift/drag ratios of 2-3 (Fig. 2). As expected, the velocity remaining at the end of the 90 deg turn is much higher, by a nearly constant value of 1.8 km/s, than for the 180 deg turn. The effect of L/D on conserving velocity is also evident in Fig. 2. For the 90 deg turn, an L/D of 3 results in about a 30% higher final velocity than for an L/D of 2. For the 180 deg turn, the effect of increasing L/D is even more dramatic and produces about a 70% increase in the final velocity.

The longitudinal distance that a vehicle can glide after completing a turn depends on the residual velocity at the end of the turn. The residual range can be calculated from relations given in Ref. 4, and is

$$s = -\frac{R_0}{2}\frac{L}{D}\ell n\left(1-\frac{V^2}{V_s^2}\right) \tag{7a}$$

which can be combined with Eq. (3b) to give

$$s = -\frac{R_0}{2}\frac{L}{D}\ell n\left[1-\left(\frac{V_i}{V_s}\right)^2 \exp\left\{\frac{-2\psi}{[(L/D)\sin\phi]}\right\}\right] \tag{7b}$$

The lateral range traversed during a turn is[1]

$$\ell = R_0\frac{L}{D}\cos\phi\int_{V_i}^{V_f}(\sin\psi)\frac{V\mathrm{d}V}{V^2-V_s^2} \tag{8}$$

where V_f is found using Eq. (3b). After integrating Eq. (3a) for the turn angle to yield

$$\psi = \frac{L}{D}\sin\phi\ell n\frac{V_i}{V}$$

and substituting for ψ into Eq. (8), the lateral range is found by numerically integrating Eq. (8), using the optimum bank angle from Eq. (6) or Fig. 1.

Both the lateral ranges and the residual ranges after turns of 90 and 180 deg are shown in Table 1 for maneuvers initiated upon entry at V_s. The lateral distances covered during both turns are very large, varying about 3000-6000 km as the L/D is increased from 2 to 3. Since the velocity at the conclusion of the 90 deg turn is much higher than after the 180 deg turn (see Fig. 2), the residual ranges for the former are from 5.6 times (at $L/D=2$) to 3.5 times (at $L/D=3$) greater. For vehicles having L/D of 2.5 or greater, at least 30% of the total lateral range is traversed after completing the 90 deg turn.

The lateral range is greatly reduced if the maneuver is initiated some time after entry. For example, if $V_i = 0.8\ V_s$ and the vehicle has an L/D of 2.5, the distance covered during a 90 deg turn is only about 1670 km and the residual range 1150 km. The total lateral range is about 2820 km, or 54% less than if the turn had been started upon entry at V_s.

Finally, the problem of achieving a global choice of landing sites is addressed. A vehicle can land at any location within a hemisphere of the entry point if it has a lateral range of 10,000 km. (Since atmospheric entry can be chosen at any point in the orbit, the vehicle having a hemispherical lateral range can land anywhere on Earth.) By equating the sum of Eqs. (7a) and (8) to the required distance, the necessary L/D can be found. The previously derived optimum bank angles were used during the turning part of the flight and a trial-and-error procedure was employed to solve the equation. The maximum L/D required to achieve global landing coverage is 3.23, which is 5% less than the value of 3.40 given by the formulation in Ref. 3. Since such high L/D are very difficult to achieve at hypervelocity speeds, the 5% reduction may be important.

Conclusions

Analytic expressions for turning maneuvers during gliding entry from circular satellite speed or lower have been presented. The longest lateral ranges and the highest residual velocities after completing the turns are achieved by beginning the turns at entry speed, before the vehicle decelerates. Lateral distances of 3000 and 6000 km can be traversed during 90 and 180 deg turns for L/D of 2 and 3, respectively. It is shown that, after completing 90 deg turns, sufficient energy remains to extend the lateral range by 33-52%. For the 180 deg turns, the residual energy is much less, but still allows gliding for distances equal to 6-14% of the lateral range. The present optimum turn calculations also show that a choice of global landing sites can be achieved with an L/D of 3.23, or a 5% lower value than obtained from previous formulations.

References

[1]Slye, R. E., "An Analytical Method for Studying the Lateral Motion of Atmosphere Entry Vehicles," NASA TN D-325, 1960.

[2]Eggers, A. J. Jr., "The Possibility of a Safe Landing," *Space Technology*, edited by H. S. Seifert, Wiley, New York, 1959.

[3]Shkadov, L. M., Bukhanova, R. S., Illarionov, V. F., and Plokhikh, V. P., "Mechanics of Optimum Three-Dimensional Motion of Aircraft in the Atmosphere," NASA TT-F-777, March 1975 (original date 1972).

[4]Eggers, A. J. Jr., Allen, H. J., and Neice, S. E., "A Comparative Analysis of the Performance of Long-Range Hypervelocity Vehicles," NACA TR-1382, 1958.